AD-A153 565 PASSIVATION ON HIGH Q ACOUSTIC STRAIN SENSOR FOR ACCELEROMETER..(U) ROCKWELL INTERNATIONAL THOUSAND OAKS CA MICROELECTRONICS RESE.. M W MOTAMEDI NOV 84 1/1

UNCLASSIFIED MRDC-41108.3FR AFOSR-TR-85-0281 F/G 20/1 NL

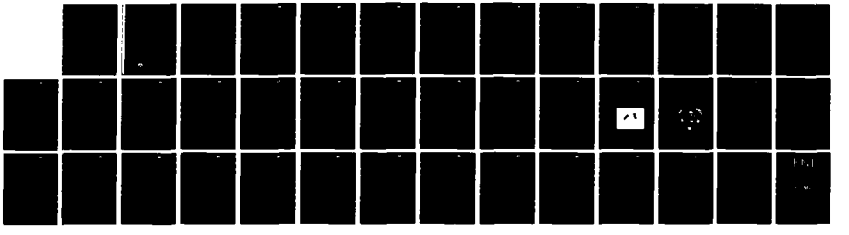

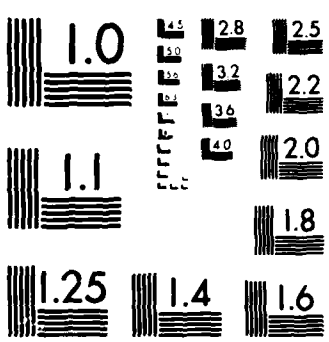

MRDC41108.3FR

MRDC41108.3FR

Copy No. 12

PASSIVATION ON HIGH Q ACOUSTIC STRAIN SENSOR FOR ACCELEROMETER

FINAL TECHNICAL REPORT FOR THE PERIOD
February 14, 1982 through July 13, 1984

CONTRACT NO. F49620-82-C-0012

Prepared for

Air Force Office of Scientific Research
Bolling Air Force Base
Washington, DC 20032

M.E. Motamedi
Principal Investigator

Microelectronics Research and Development Center
Rockwell International
1049 Camino Dos Rios
Thousand Oaks, CA 91360

NOVEMBER 1984

Rockwell International

AD-A153565

UNCLASSIFIED
SECURITY CLASSIFICATION OF THIS PAGE

REPORT DOCUMENTATION PAGE

1a. REPORT SECURITY CLASSIFICATION Unclassified	1b. RESTRICTIVE MARKINGS
2a. SECURITY CLASSIFICATION AUTHORITY	3. DISTRIBUTION/AVAILABILITY OF REPORT Approved for public release; distribution unlimited.
2b. DECLASSIFICATION/DOWNGRADING SCHEDULE	
4. PERFORMING ORGANIZATION REPORT NUMBER(S) MRDC41108.3FR	5. MONITORING ORGANIZATION REPORT NUMBER(S) AFOSR-TR- 0281
6a. NAME OF PERFORMING ORGANIZATION Rockwell International Microelectronics Research and Development Center 6b. OFFICE SYMBOL (If applicable)	7a. NAME OF MONITORING ORGANIZATION NPCSR/NE
6c. ADDRESS (City, State and ZIP Code) 1049 Camino Dos Rios Thousand Oaks, CA 91360	7b. ADDRESS (City, State and ZIP Code) BLDG 410 BAFB DC 20332-6448
8a. NAME OF FUNDING/SPONSORING ORGANIZATION Air Force Office of Scientific Research 8b. OFFICE SYMBOL (If applicable) NE	9. PROCUREMENT INSTRUMENT IDENTIFICATION NUMBER Contract No. F49620-82-C-0012
8c. ADDRESS (City, State and ZIP Code) Bolling Air Force Base Washington, DC 20032	10. SOURCE OF FUNDING NOS. PROGRAM ELEMENT NO: 61102F; PROJECT NO: 3005; TASK NO: B2; WORK UNIT NO:
11. TITLE (Include Security Classification) PASSIVATION ON HIGH Q ACOUSTIC STRAIN SENSOR FOR ACCELEROMETER (U)	
12. PERSONAL AUTHOR(S) Motamedi, M. Ed	
13a. TYPE OF REPORT Final Technical Report 13b. TIME COVERED FROM 02/14/82 TO 07/13/84	14. DATE OF REPORT (Yr., Mo., Day) NOVEMBER 1984 15. PAGE COUNT 39
16. SUPPLEMENTARY NOTATION	

17 COSATI CODES		
FIELD	GROUP	SUB. GR.

18. SUBJECT TERMS (Continue on reverse if necessary and identify by block number)
Accelerometer, Frequency Stability, Interface and Layered Waves, Surface Effects, Passivation Films, SiO_2, AlN, Y_2O_3.

19. ABSTRACT (Continue on reverse if necessary and identify by block number)

The objective is to study the passivation effects on the frequency stability of SAW resonators. Cantilever SAW accelerometers based on the SAW resonator to be sensing element of acceleration is considered for a wide spectrum of Air Force applications. To produce the desired accuracy, a quartz beam is designed with the required sensitivity and a size adequate for the resonator structure. A theory of interface waves is developed for the purpose of material and thickness selection of passivation layers. Preliminary results indicated that Y_2O_3 (yttrium oxide) and AlN (aluminum nitride) were the best materials for passivation of SAW resonators.

20. DISTRIBUTION/AVAILABILITY OF ABSTRACT UNCLASSIFIED/UNLIMITED ☒ SAME AS RPT. ☐ DTIC USERS ☐	21. ABSTRACT SECURITY CLASSIFICATION Unclassified
22a. NAME OF RESPONSIBLE INDIVIDUAL	22b. TELEPHONE NUMBER (Include Area Code) 22c. OFFICE SYMBOL

DD FORM 1473, 83 APR EDITION OF 1 JAN 73 IS OBSOLETE.

UNCLASSIFIED
SECURITY CLASSIFICATION OF THIS PAGE

TABLE OF CONTENTS

A1

LIST OF FIGURES

LIST OF FIGURES

SUMMARY

The ultimate goal of this investigation is to obtain resonator structures with improved long-term stability characteristics, so that these devices can meet the performance requirements for "moderate accuracy" accelerometers. This level of accuracy is required for a wide spectrum of Air Force applications, including tactical missiles and aircraft. This level of accuracy can be met by SAW accelerometers.

The objective of this work is to study the passivation effects on the frequency stability of SAW resonators. Cantilever SAW accelerometers based on the SAW resonator to be sensing element of acceleration is considered for a wide spectrum of Air Force applications. To produce the desired accuracy, a quartz beam is designed with the required sensitivity and a size adequate for the resonator structure. A theory of interface waves is developed for the purpose of material and thickness selection of passivation layers. Preliminary results indicated that Y_2O_3 (yttrium oxide) and AlN (aluminum nitride) were the best materials for passivation of SAW resonators.

1.0 INTRODUCTION

Inertial sensors are used in airborne weapon systems such as cruise and MX missiles for navigation guidance and flight control.[1] The cruise missiles use the force-rebalance accelerometer in which the current waveforms for electro-magnetic forcing of the proof mass are digitized as pulses. Such accelerometers require precision electronics, machining and assembly, and hence the cost is high. In addition, the warm-up time for stabilization is long (typically in minutes).

Accelerometers are transducers which convert sensed acceleration to analog or digital signals. They are used in a wide variety of applications, such as in sensing seismic, kinesthetic and vibrational motions; but the most stringent requirements for these devices occur in their applications for guided missiles.

The development of guided missiles in the 1930's and 1940's required the development of accurate accelerometers for steering and stability augmentation. This led eventually to the development of accelerometers for autonomous inertial navigation of missiles, aircraft and ships. They are also used for autopilots and smoothing for navigational mechanizations using satellite data.

The technological approaches for accelerometers of the 1930's and 1940's are still in use today. These include integrating gyroscopic accelerometers of the type used on the German V-2 rockets.[2] Refinements to these approaches have improved these instruments in many respects, but they have not made them inexpensive. They require precision machining and assembly of many mechanical parts, which can not be accomplished at low cost. Typical unit cost for accelerometers used in inertial navigation range from a few thousand dollars to tens of thousands of dollars.

There is a constant need for less costly accelerometers, especially for applications such as cruise missiles and tactical missiles,[3] for which large numbers of accelerometers are required. Many technological approaches have been proposed for meeting this need. These include "vibrating string," laser,[4] pie-

zoresistive,[5] piezoelectric[6] and acoustic[7,8] accelerometers. All of these approaches use a "proof mass" which is connected to the host vehicle by means of a stress sensor. The stress sensor measures the force applied to the proof mass, which is proportional to the sensed acceleration of the host vehicle. These are called "open-loop" sensors, because the force is not applied by a precision servo loop, as in the case of the gyroscopic and pendulous accelerometers. These two approaches are shown in Fig. 1.

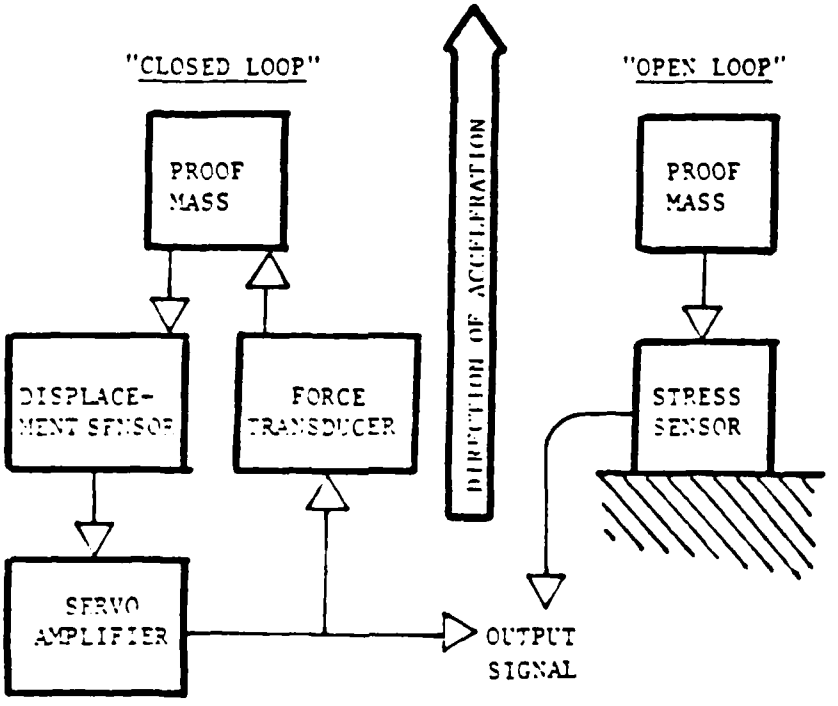

Fig. 1 Functional schematic of accelerometers.

An open-loop accelerometer is like a "mass spring" system, in which the deflection of the spring is a measure of the acceleration applied to the mass.

Like a mass-spring system, it is limited in accuracy by the linearity of displacement (strain) with the applied force (stress). This problem is avoided in the closed-loop accelerometers by designing a very stiff servo, which greatly limits the effective compliance. The linearity of the closed-loop accelerometers depends almost entirely upon the linearity of the servo loop. (This does require precision fabrication to achieve the required linearity, which is where the high cost comes in.)

Stress/strain linearity of the open-loop accelerometers can be improved by increasing the effective spring stiffness. This limits strain to a range of better stress/strain linearity, but it also limits the total signal variation due to input acceleration. This sacrifices the signal-to-noise ratio, and increases the sensitivity to other strain effects - such as thermal strain.

The sensitivity to thermal effects can be improved by using two sensors in a "push-pull" configuration, as shown in Fig. 2. In this configuration, the acceleration applied to the proof mass equals the difference of the accelerations applied at the two ends. Consequently, any common effect such as temperature will not effect the output of such a device.

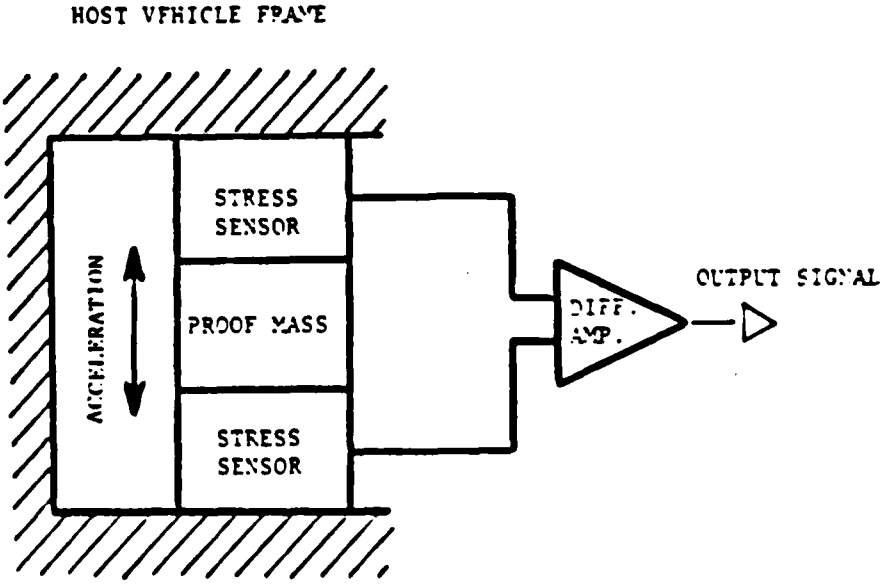

Fig. 2 Functional schematic of "push-pull" configuration.

For example, in the vibrating-string accelerometer a vibrating string is attached to each end of the proof mass, with the other ends attached to the host vehicle. The vibrating string is a stress sensor. Its fundamental vibrational frequency is proportional to the square root of the tension (stress) applied at the ends. This nonlinearity can be eliminated by using a tension servo at one end to control the sum of the vibrational frequencies of the two strings to a constant value. With the approach then the difference of the two vibrational frequencies will satisfy the following chain of relationships:

$$f_1 - f_2 = \frac{f_1^2 - f_2^2}{f_1 + f_2}$$

$$\propto T_1 + T_2$$

$$= F$$

$$\propto a$$

where

$\propto$ stands for "is proportional to"

f_i is the vibrational frequency of the ith string, (i = 1, 2)

T_i is the tension in the ith string, (i = 1, 2)

F is the net force applied to the proof mass

a is the acceleration of the proof mass, which must equal to acceleration of the host vehicle.

The laser accelerometer operates in a similar manner, with the vibrating strings replaced by sections of material whose optical properties are stress-dependent. These sections are in the paths of laser beams, which are then combined optically to provide an output signal whose frequency is proportional to the difference of the stresses applied at opposite ends of the proof mass.

Neither the vibrating string accelerometer nor the laser accelerometer offers much cost advantage over the closed-loop accelerometers. They all require precision servos and precision fabrication methods which are relatively expensive. The piezoelectric, piezoresistive and acoustic sensors do offer the advantage that they are compatible with the low-cost fabrication technologies which have evolved for integrated circuits. These could offer a significant improvement in fabrication costs for accelerometers - perhaps one or two orders of magnitude improvement in fabrication cost.

The piezoelectric sensor is essentially a strain-to-charge transducer. Because the impedance of the charge circuit is never infinite, there is always some charge leakage that gives less-than-infinite memory for this type of accelerometer. This causes the output to decay toward zero over periods of hours or days. Therefore, the piezoelectric accelerometer can not be used for friction (leveling) of an inertial system. This greatly limits the usefulness of piezoelectric accelerometers for inertial applications.

Piezoresistors are strain-to-resistance transducers. They also exhibit significant nonlinearities, temperature sensitivities and noise with 1/f power spectral density. These problems have limited the accuracy of piezoresistive accelerometers to about 1000 ppm.[5] Since these problems are associated with the physics of the piezoresistive materials, this may be a fundamental limitation of this approach.

Acoustic accelerometers use the strain sensitivity of acoustic resonances within the propagating medium to convert strain information to acoustic signal frequencies. These devices have the same problems with thermal sensitivity and nonlinearity as the piezoresistive devices, but they have much lower noise levels.

Surface acoustic wave (SAW) technology offers an approach for an inherently digital acceleration sensor with no precision electronics and machining assembly. This technology uses established planar photolithography for low-cost fabrication. The associated electronics contains only one active element

(transistor). Simplicity makes this an attractive candidate for digital sensor applications in future missiles and manned and unmanned aircraft.

For "moderately" accurate inertial guidance systems, the integrated errors in accelerometers in positional accuracy are typically 1 NM/h. SAW-resonator accelerometers typically possess a dynamic range of 1×10^6 and a full-scale frequency deviation of 200 ppm corresponding to 10 Gs of acceleration.

Recent studies involving the double integration of SAW accelerometer indicate a position accuracy of 200 meters/h (or 0.1 NM/h) is achievable.

Long-term bias stability in single crystal SAW accelerometers is typically 0.5% full scale/yr. Dual crystal sensors are considerably better, typically 0.01% full scale/yr. Current research is aimed at improving the long-term stability of this sensor to achieve the ultimate goal of 0.001% (full scale) or 100 mG/G/yr.

1.1 The SAW Resonator

The SAW resonator is a strain-to-frequency converter. It has the structure shown in Fig. 3. This consists of an interdigital transducer between reflective gratings on a piezoelectric (quartz) substrate. A signal applied to the transducer launches Rayleigh mode waves along the surface of the substrate which are coherently reflected by the gratings.

Longitudinal strain applied to the resonator cavity will cause a proportional change in its resonant frequency. This provides a bit rate frequency output which is proportional to strain input. This relationship forms the basis of the simplest SAW accelerometer, as shown in Fig. 4. This is a simple cantilever beam configuration. Acceleration applied at the clamped end is transmitted to the proof mass at the free end through bending stress. The resulting surface strain along the SAW resonator causes a frequency shift which is proportional to the applied acceleration.

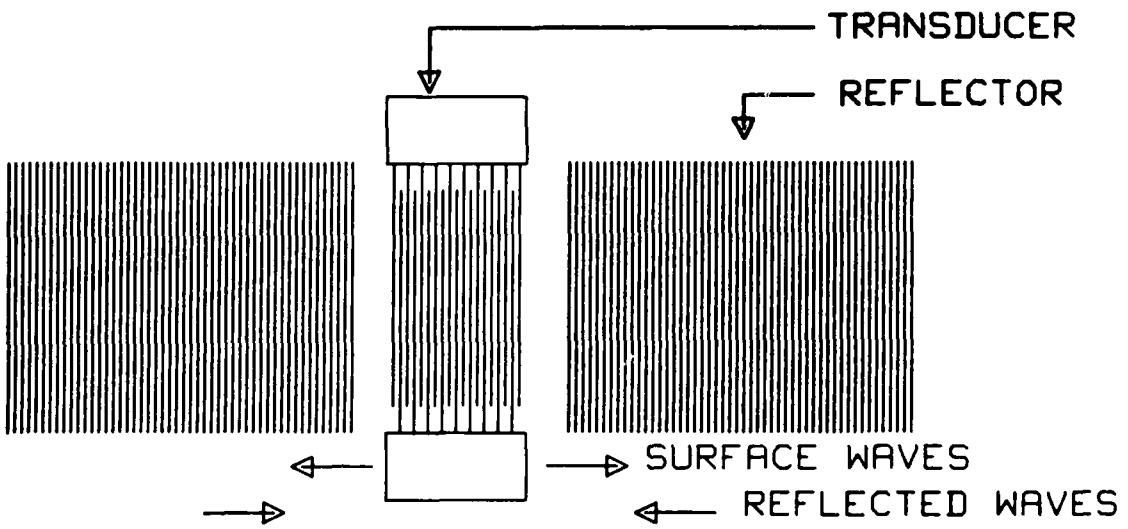

Fig. 3 Electrode structure of SAW resonator cavity.

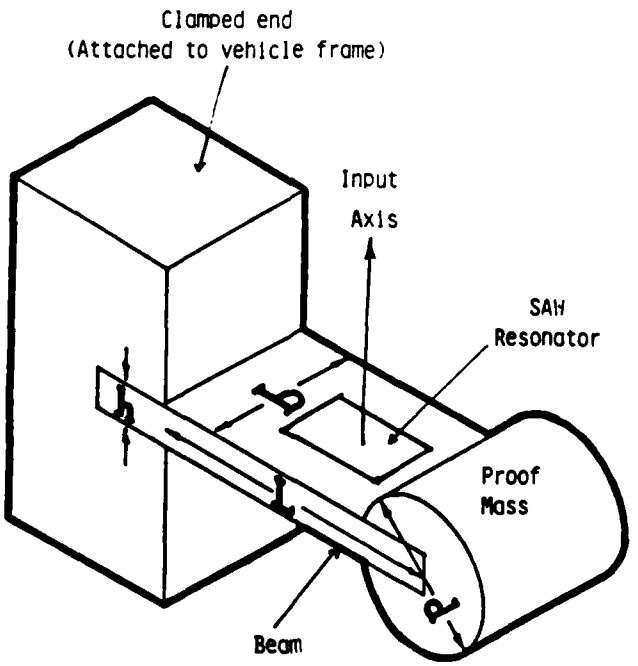

Fig. 4 Simple cantilever SAW accelerometers.

1.2 Cantilever Accelerometer

Planar cantilever devices show promise for meeting these needs with an open-loop accelerometer without bearings or points of wear. By using established planar fabrication techniques, it is possible to make an integrated circuit containing strain-sensitive elements on a substrate which acts as a clamped plate or beam. Acceleration forces on this device will cause surface strains that are sensed and processed by the electronic circuit. This type of accelerometer can potentially be inexpensive. It uses little power and can be made small and reliable.

Ideally, the acceleration sensor should be able to operate over the full operational range of ambient temperatures without temperature control. Depending upon the systems application, this temperature range can be as great as 179°C for Class IV avionics, or as small as 109°C for Class I avionics. Conventional accelerometers are not likely to perform as well as cantilever devices over such large temperature variations, because their design depends upon different properties of different materials, and these are difficult to maintain in the proper relationship over large variations in temperature.

Accelerometers are needed for guidance, stability augmentation, and navigation of guided missiles and aircraft. For applications in future tactical systems, these accelerometers should be less expensive, more reliable, and smaller than the floated gyroscopic accelerometers, drag cup velocity meters or electromagnetic force-rebalance accelerometers now in use. For missiles and other applications where rapid reaction is a necessity, these devices need to be able to operate without first being thermally stabilized at a given operating temperature.

A set of resonators were tested simultaneously at room temperature or elevated and/or programmed temperatures for characterizing the long-term stability.

Similar aging data are taken from the SAW oscillators where the resonator is in the feedback loop. Characterizing SAW oscillators and collecting all the data for both short-term and long-term stabilities, will give us a chance to

choose the SAW oscillators with required specifications to construct a desired SAW accelerometer sensor.

To optimize the design of the SAW accelerometer, we prepared the preliminary test results for dynamic testing of a mechanical cantilever beam when the SAW oscillator is bonded on the surface of the beam. The generated surface strain as a result of the acceleration was transferred to the resonant frequency characteristics of the SAW oscillator. The collected data were used for preliminary estimation of the sensitivity and scale factor.

1.3 Quantization of SAW Accelerometer

The bit quantization for a SAW accelerometer is in the same range as those of high precision accelerometers. For a SAW accelerometer with 320 MHz frequency and proof mass loading to produce 200 ppm strain at 20 G input acceleration, the bit quantization will be

$$\frac{(20\ \text{G})\ (32\ \text{fps/s/G})}{(320 \times 10^{6}\ \text{bit/s})(200 \times 10^{-6}\ \text{p/p})} = 0.01\ \text{fps/bit} \quad .$$

The short-term stability of the SAW resonator (over periods of seconds) is in the order of 0.1 parts per billion. For the above example, this gives a comparable short-term bias stability of

$$\frac{10^{-4}\ \text{ppm}}{200\ \text{ppm}/20\ \text{G}} = 10\ \mu\text{G} \quad ,$$

this gives a dynamic range of

$$\frac{20\ \text{G}}{10\mu\ \text{G}} = 2 \times 10^{6} \quad .$$

1.4 Present SAW Technology

At the present time, short-term frequency stability of SAW resonators is comparable to that of bulk-wave crystal oscillators. Long-term stability of SAW resonators is not as good as that of bulk wave crystal oscillators. SAW resonators typically have short-term (seconds to minutes) frequency stability with root Allen variance in the order of 10^{-10} parts/part of the resonant frequency and long-term aging rates in the order of 10^{-8} part/part/day. The long-term aging rates for conventional quartz resonators are in the order of 10^{-10} part/part/day.

Short term stability for tactical missile application (flight time less than 20 min) is not a significant problem. A variation of 10^{-10} of 320 MHz would equal 0.032 Hz. With a quantization of 0.01 fps/bit, this would equal 10 μG acceleration error. Errors in inertial navigation systems behave like a resonator with a natural period of 84 min.

Performance limitations due to long-term frequency stability are a more serious problem for bias stability of a SAW accelerometer. The dual SAW sensor aging rates in "ovenized" environment are in the order of 10^{-8}/yr. For a SAW accelerometer with 320 MHz frequency and 0.01 fps/bit quantization, this would amount to about 0.001 G/yr:

$$\frac{(10^{-8}/\text{yr})(320 \times 10^{6}\ \text{cycle/s})(0.01\ \text{fps/cycle})}{(32\ \text{fps/s/G})} = 0.001\ \text{G/yr} \quad .$$

This meets most of the performance characteristics of the accelerometer. Table 1 contains a representative set of accelerometer performance requirements for "moderate" accuracy inertial navigators. However, for SAW sensor in the unovenized condition, the aging rates are in the order of 10^{-7}/yr. Hence, the bias stability is now 0.01 G/yr (or 10,000 μG/yr) which does not meet the specification of tactical missiles.

Table 1

Tactical Accelerometer Requirements
(From Air Force and Army)

Long Term Bias Stability	500-1000	μG/yr
Linearity	5-10	$\mu G/G^2$ quadratic
	3-4	$\mu G/G^3$ cubic
Symmetry	2	μG/G
Operating Temperature	-40, +100	°C
Full Scale Output	20	G
Integrated Error Rate	1	Mile/h
Reaction Time	1	min
Cross-Axis Coupling	50	Arc-s
Frequency Response	100	Hz
Dynamic Range	10^6	Numbers
Vibration	8-10	G-rms

The SAW resonator has a length in the order of 5 mm and can fit easily into small instrument design. Its weight is practically insignificant, and its power requirements are in the order of a few milliwatts of dc power. Its electronic complement is minimal. Because it has a low thermal mass, it can be heated rapidly with little power. Temperature control may be required; sensitivity to temperature is about 34 parts per billion per $°C^2$ (quadratic).

2.0 TECHNICAL PROGRESS

2.1 Background

During the past several years SAW sensors were fabricated and tested in our laboratory for bias stability and frequency response. The test results were excellent and matched very well with design predictions. The SAW dual crystal oscillator frequency stability determines the noise floor or bias stability of the SAW sensor. Directly related to this is the sensor instantaneous dynamic range. The full scale output of the sensor is typically 200 ppm and assuming a noise floor of 1×10^{-10}, the dynamic range is typically 1×10^{6}.

Associated with this study was an evaluation of integrated noise floors. An important potential application of the SAW sensor is for inertial navigation and guidance. Consider the output of the sensor being a train of pulses whose count per second is proportional to acceleration. To determine velocity, V, from such a sensor, the acceleration count must be integrated. This is equivalent to summing the total number of counts and scaling according to the sensor gage factor and count duration.

Shown in Fig. 5 is the actual count output of a SAW sensor when measured by a counter with a 1 s gate time. The difference frequency was 60 kHz which has been subtracted out and only the deviation in the difference frequency (1 Hz) is shown. Summing the counts results in the velocity count (10 Hz) as a function of time shown. This curve represents the area under the acceleration-frequency curve. Performing another summation as a function of time results in the curve for displacement (4000 Hz). The scale factor was 200 ppm/G or approximately 769 Hz/m/s.^{2} The integrated velocity error for the 1000 s time period shown was typically less than 0.013 m/s, and the position error was typically less than 5.2 meters. As expected, the integrated error is closely related to the integration time, and this is dependent upon the actual mission time or time for which no other guidance data is available.

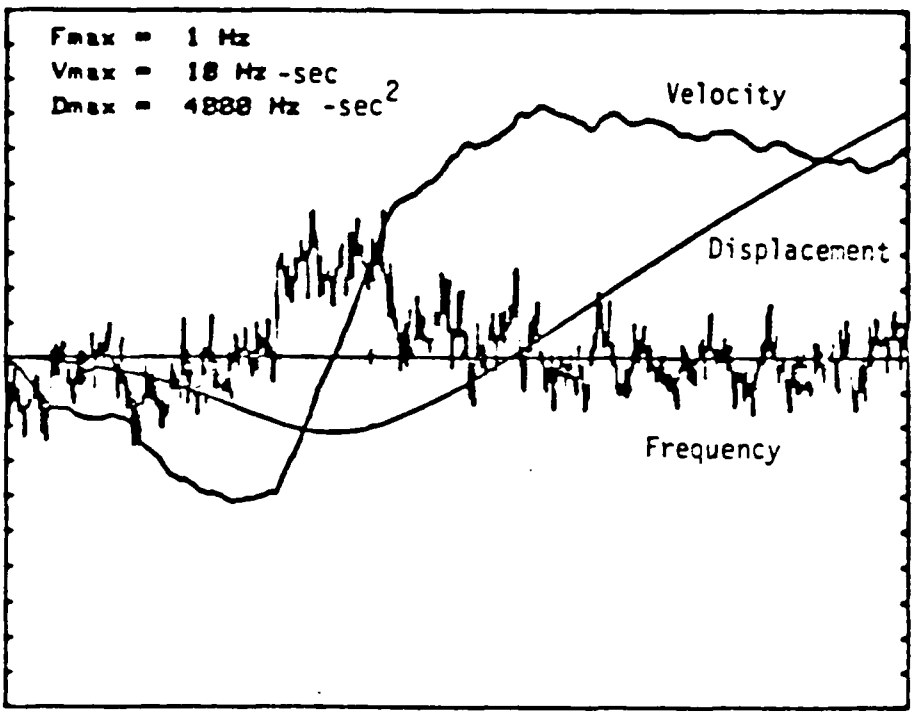

Fig. 5 Measured count output of a SAW dual crystal sensor vs time. Total time was approximately 18 min with a 1 s gate time. Also shown is the computed velocity from integrating once as well as the displacement as a result of integrating the counter output twice.

Studies of the temperature tracking of dual SAW resonator crystals were made and showed that the cycling of temperature over a suitable range was required while simultaneously monitoring bias stability or the difference frequency of SAW sensors.

A computerized measurement system was designed using an automatic frequency counter, a progammable environmental chamber, and a scanner data acquisition system. Software was designed to control temperature and read the frequency of oscillators simultaneously. Tests results for two SAW oscillators configured around a sensor crystal are shown in Fig. 6. The results were plotted during data acquisition as histograms. The top two traces showed oscillator

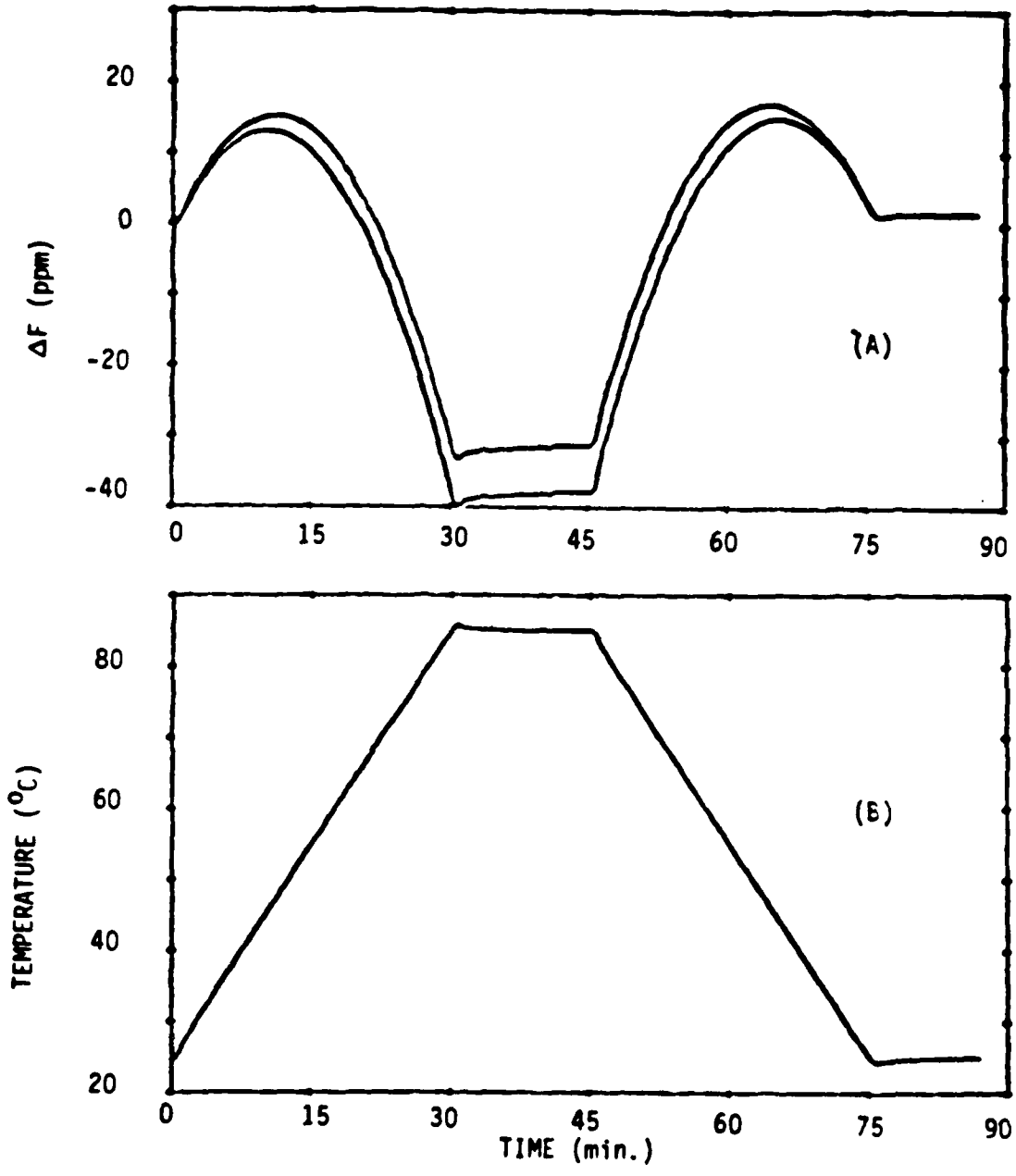

Fig. 6 Histograms of (a) frequency and (b) temperature for a SAW sensor.

frequency, and the bottom trace showed temperature in the environmental chamber. The chamber was programmed to increase temperature 2°/min until 80°C is reached. The temperature was held for 15 min and then reduced at -2°/min until 25°C was reached. The cycle was then repeated as desired.

Methods of temperature compensating SAW oscillator-sensors were investigated. Design studies indicated temperature compensation circuitry, configured as shown in Fig. 7, could maintain the sensor frequencies provided a shift could be introduced which was opposite to that of the surface wave crystal, in this case a parabolic temperature characteristic. Several circuits were designed using varactor diode phase shifting networks.

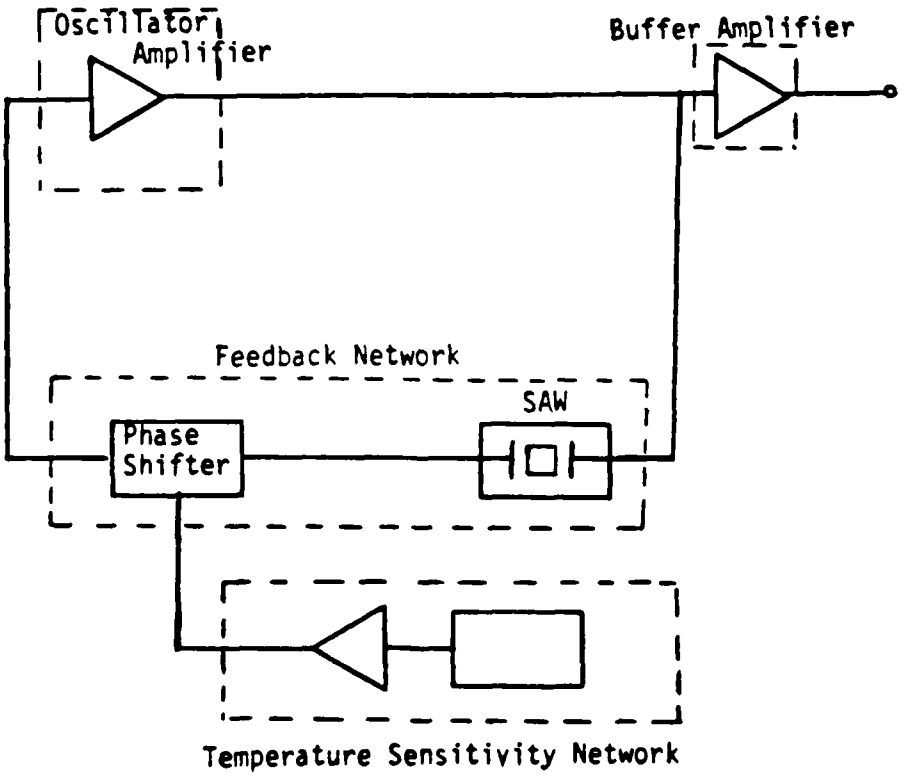

Fig. 7 Block diagram of temperature compensated SAW sensor.

To test the design feasibility, experimental temperature compensated oscillators were built. Surface wave two-pole crystal filters were used as feedback elements in order to extend the temperature range over which the oscillators could be compensated. Prototype crystals operating nominally at 198 MHz were fabricated and placed in oscillator feedback circuits which contained parabolic phase shifting networks.

Frequency vs temperature for a test circuit over the range 0-100°C is shown in Fig. 8. Multiple scans are shown indicating hysteresis which was due to unsealed crystal units in these prototype circuits. Nevertheless, temperature compensation is evident and the frequencies were held to within 35 ppm as shown by the dashed limits. A sharp drop in frequency with increasing temperature at 45-50°C was due to a higher-order resonator transverse mode in the SAW two-pole crystal phase slope. Improvements in the crystal design to eliminate transverse modes and proper sealing of the crystals to eliminate hysteresis is expected to result in compensation of 10 ppm over the temperature range -30-100°C.

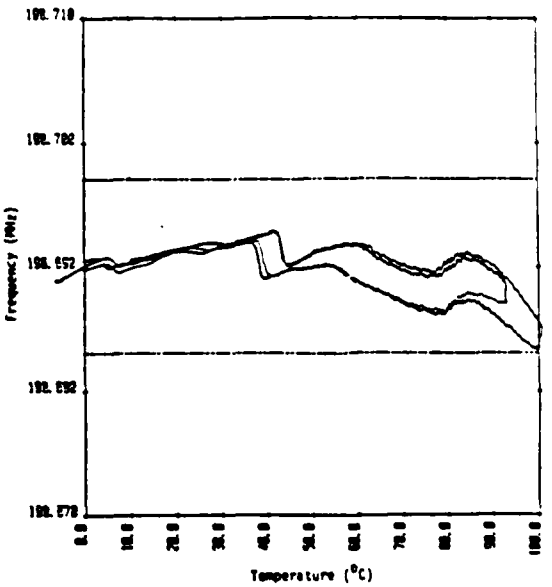

Fig. 8 Frequency as a function of temperature for prototype SAW sensor.

Shown in the photograph of Fig. 9 are quartz accelerometer beams after etching. In this case, five beams are etched into a 1 in. × 1 in. × 0.010 in. quartz wafer. Etched beams are in the shape of a hammer-head where the head of the beam acts as a proof-mass. The beams are connected by small unetched bridge sections and a simple break of the connecting bridges separates the beams. After separation, the beams are ready for processing of SAW resonator patterns on top and bottom surfaces of the beam. Also shown in Fig. 9 is a single beam mounted on a 16-pin dual in-line hermetic package using a teflon clamp fixture.

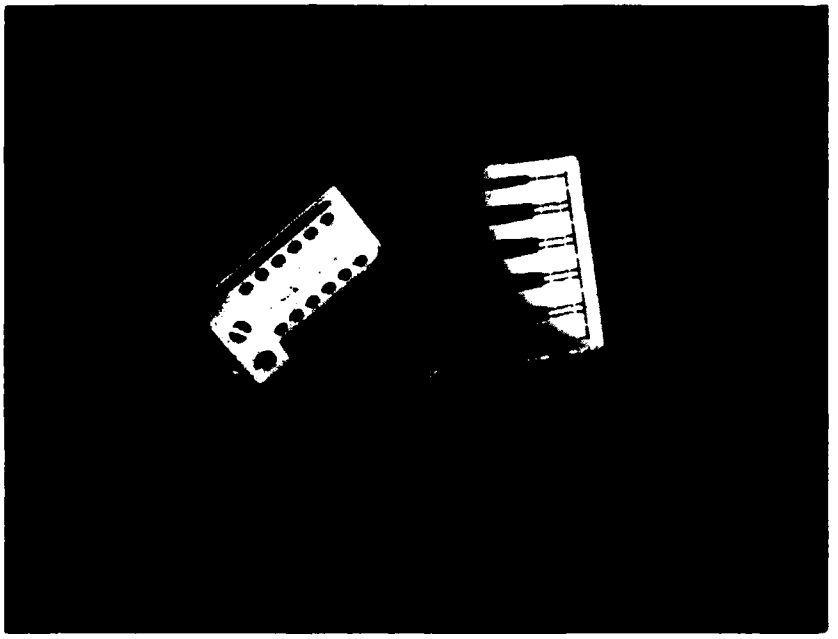

Fig. 9 Photograph of 5 hammer-head cantilever beams and teflon clamp for mounting the cantilever beams.

Ceramic boards containing the hybrid oscillator circuitry (not shown in Fig. 9) are mounted on edge along both sides of the beam.

Figure 10 shows a typical completed SAW oscillator with all required circuitry mounted on ceramic substrate inside a standard TO-8 package. After connecting the SAW resonators (on the beams) to the hybrid circuits, the entire package is sealed under vacuum using a resistance welding sealer. A special RF shielded box with OSM connectors and 50-ohm transmission lines were designed for dual SAW accelerometer packaging.

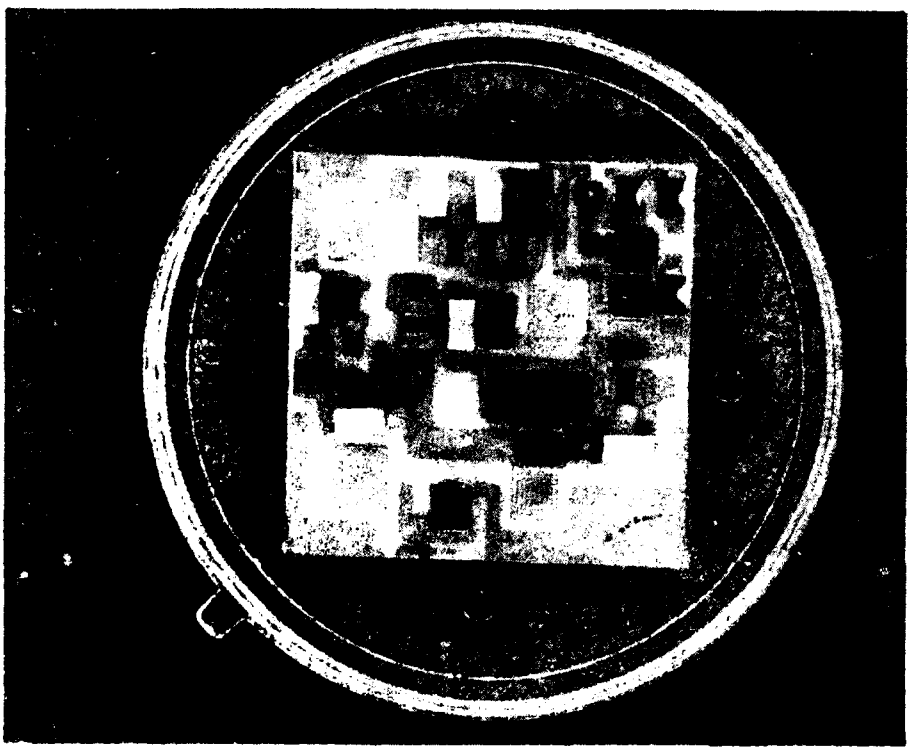

Fig. 10 A completed oscillator circuit on ceramic substrate and mounted inside TO-8 package.

2.2 Theory of Interface Waves

Acoustic wave at a free surface of a homogeneous isotropic solid medium was first discovered by Lord Rayleigh[9] in 1887 for predicting the propagation of seismic waves along the surface of the earth. Ewing, Jardetzky and Press[10] extended Rayleigh's work to layered isotropic media. Since most of the crystals are anisotropic, in 1970 Lim and Musgrave[11] studied wave propagation at boundaries between two similar anisotropic media. This extended the work of Stoneley[12] to anisotropic media.

The more recent investigations in acoustic wave propagation are directed toward applications to ultrasonic devices, rather than to seismic phenomena. The work of Farnell and Adler[12] is specifically aimed at ultrasonic applications in which the thickness of the layers is small compared to a wavelength. The results point out the existence of single-mode Rayleigh waves at the boundary of half spaces with a single layer of dissimilar material. Stoneley waves[12] also provide a single mode acoustic wave propagation at a boundary between dissimilar materials, but these waves require a thickness of several wavelengths on either side of the boundary, hence, this requirement is not desirable for the accelerometer application.

The wave equations for elastic interface waves can be defined in terms of a displacement vector U, which is a function of position within the medium. The boundary conditions at interfaces can then be expressed in terms of continuity of the particle displacements and the stresses. For these purposes, it is simpler if the coordinates are chosen such that the boundaries are normal to one of the coordinate axes and the propagation direction is parallel to another of the coordinate axes. If we let the first coordinate axis correspond to the direction of propagation and the third axis be normal to the interface, then the coordinates of the displacement vector can be expressed in the following form:

$$U_j = \sum_{n=1}^{3} C_n \alpha_{nj} e^{ijbx_3} e^{ij(x_1 - vt)} \quad , \quad j = 1,2,3$$

where x_1 is the direction of propagation. In general, the amplitude, C, displacement vector, α, and decaying constant, b, can be complex value. The solution is subject to the boundary conditions. These conditions are used for each interface wave to determine the constants C, b, and α.

The multiple-boundary conditions are shown in Fig. 11 for the cantilver sensor configuration. These amount to requiring continuity of displacement and stresses at the solid/solid interfaces and zero stress on the surfaces. The solutions obtained depend upon the relative thicknesses of the layers, as well as density and elastic tensors of the materials. In the limiting case, as the thicknesses of the outer layers (I) or (III) approach zero and the thickness of the inner layer (II) approaches infinity, the solution is indeed the normal Rayleigh wave on a free surface.

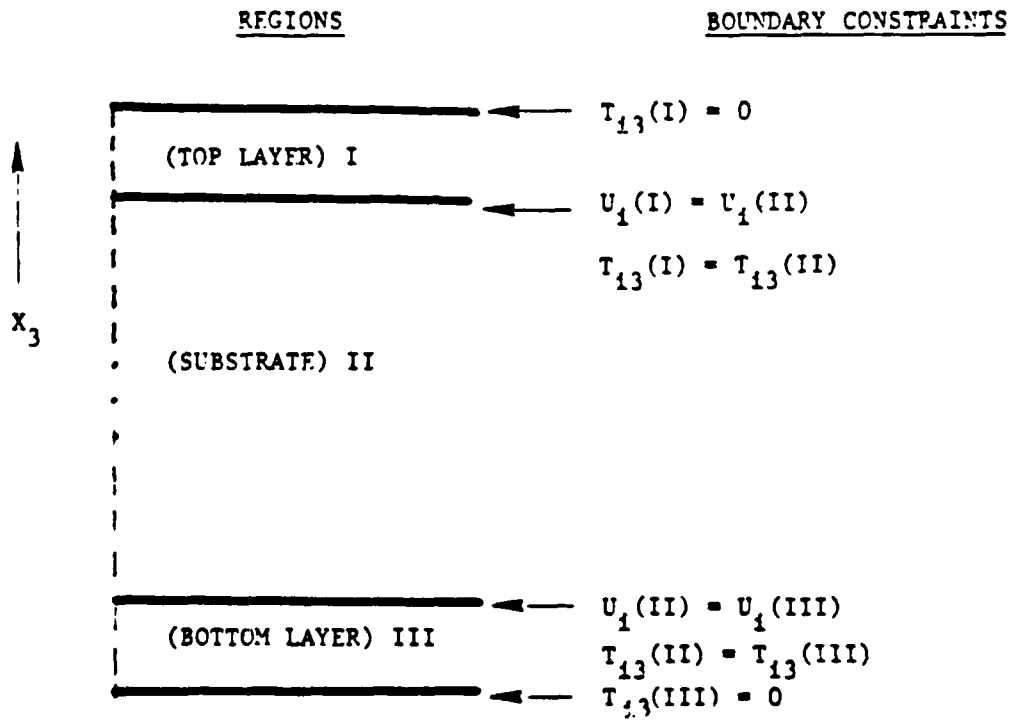

Fig. 11 Boundary conditions on displacements U and stresses T for layered cantilever SAW accelerometer.

We are seeking a solution which had independent Rayleigh modes at the top and bottom surfaces, so that we can use the difference of the two resonator frequencies as a measure of the differential strain. This can be achieved by making the thickness of the middle layer on the order of ten wavelengths or greater. Figure 12 is a plot of the two components of displacement amplitude versus depth for the first Rayleigh mode in isotropic media. It shows very little effect beyond about two wavelengths into the surface. Consequently, we can consider each half of the cantilever beam as an independent semi-infinite region for propagation of Rayleigh waves, and consider just the effect that the top layer will have upon the character of the Rayleigh waves.

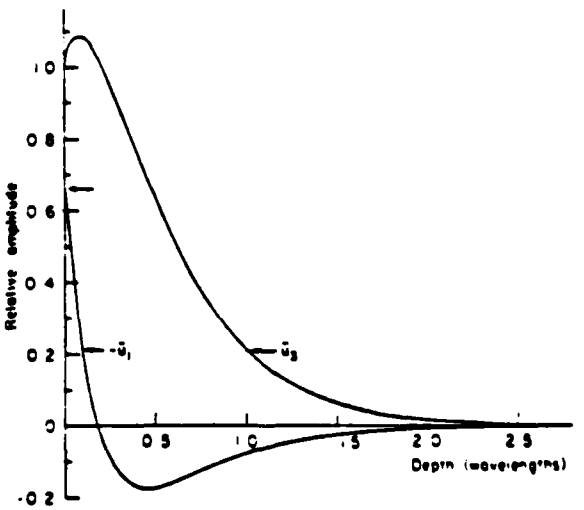

Fig. 12 Relative amplitude of normal (U_3) and tangential (U_1) displacements in normal Rayleigh wave vs depth.

The density and elastic tensors of the materials in the layer and the substrate determine the characteristics of the wave solutions, such as phase velocity and group velocity, and the numbers of solutions. For sufficiently thin layers, the solution still exists for a single Rayleigh mode. Figure 13 is a plot of the interface wave velocities versus thickness of the top layer of gold on a quartz substrate. This shows the existence of a single Rayleigh mode for kh less than 0.6. This data is of particular interest to the problem at hand, because quartz substrates are used in most stable SAW resonators, and are proposed for the accelerometer application. The reference does not contain the associated displacement curves, but it does contain the displacement curves for gold on fused quartz, which is shown in Fig. 14. These show that the amplitudes of the displacement at the surface is less than the amplitude at the solid/solid interface, which is desired for reducing the sensitivity to surface contamination.

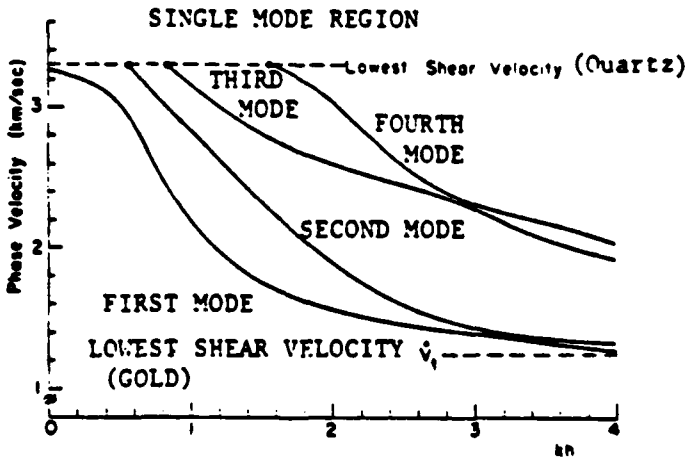

Fig. 13 Rayleigh interface wave velocities for gold layer on quartz substrate.

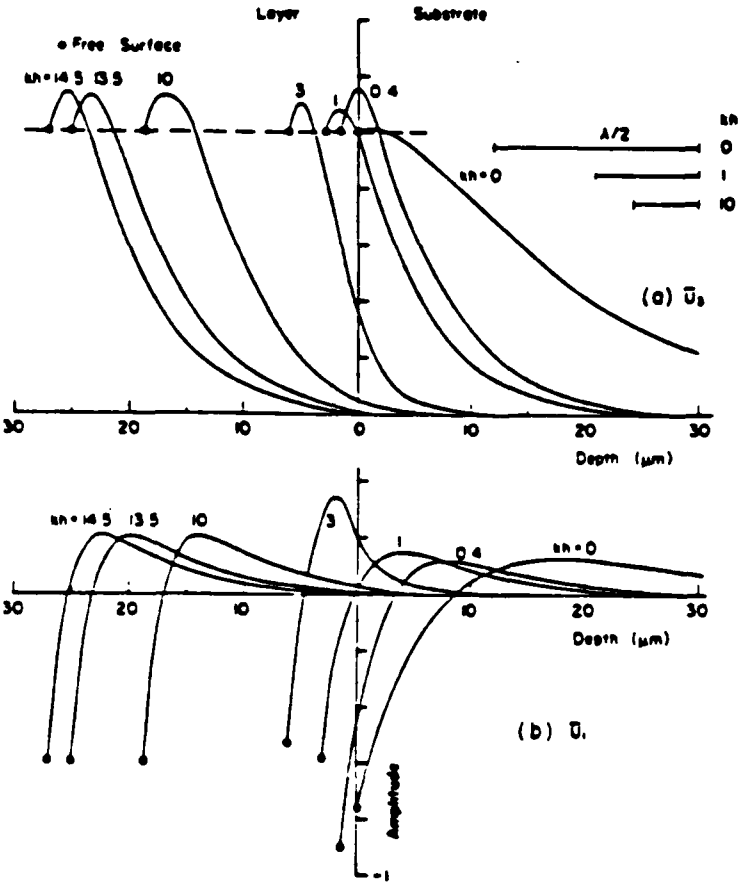

Fig. 14 Relative amplitudes of Rayleigh interface wave displacements versus depth, for various values of kh = (wave number) × (height of layer) gold on fused quartz at 100 MHz.

In general, the normal Rayleigh wave is "stiffened" by the layer if it increases the Rayleigh velocity, and "loaded" if it decreases the Rayleigh velocity. Stiffening generally results when the Rayleigh velocity of the material in the thin layer exceeds that of the material in the substrate. For example, the Rayleigh velocity is 1 km/s in gold and 3 km/s in quartz. The effect of loading on the Rayleigh phase velocity can be seen in Fig. 13. In the examples

given by Farnell and Adler[14] the displacement amplitude decreases toward the surface in both stiffening and loading layers. It appears from this that either case should improve the insensitivity of resonators to surface contamination.

2.3 Design and Evaluation

The approach for initial design of a layered resonator will be to deposit a layer on an existing SAW resonator substrate. Selection of the material for the covering layer will require theoretical investigations of the expected influence on wave propagation properties, scattering at the grooves and the function of the interdigital transducer, as well as consideration of compatible fabrication processes. Dielectric materials would be preferable for the top layer, because they can be deposited over the entire surface without steps to prevent shorting of the interdigital electrodes. Conducting material should be considered in the theoretical investigation, in order to provide a wider choice of materials. However, the use of a conducting material as a covering layer is not practical. It would require a dielectric barrier to prevent shorting of the interdigital electrodes, also. The thickness of the top layer should be on the order of 0.1 wavelengths of the first Rayleigh mode, in order to maintain a single resonant mode.[13] For resonant frequencies on the order of 100 MHz, this requires a layer of about 3 micro-meters thickness. This is a reasonable thickness for such fabrication methods as magnetron rf sputtering. The fabrication processes for producing the interdigital transducers and reflective gratings are well established at the Rockwell Microelectric Research and Development Center.

2.4 Fabrication Methods

The objective of testing is to ascertain the effectiveness of the proposed approach. The purpose of the proposed resonator design is to obtain better long-term frequency stability than that of SAW resonators. The layered structure is intended to give improved insensitivity to surface contamination. The sensitivity to surface contamination can be evaluated by purposely applying a controlled thickness of a known material to "contaminate" the surface. One

possible method is to spin on a monomolecular layer of a contaminant to the resonator surface to achieve a controlled uniform thickness. The sensitivities can be compared to those obtained with a homogeneous SAW resonator, to determine the benefit resulting from the layered structure.

Testing of aging effects on resonant frequencies must include the strain variations that a resonator would experience in the accelerometer application. "Strain aging" of test resonators can be accomplished by vibration of a cantilever-mounted resonator at the resonant frequency of the cantilever beam, to attain strain variation near the expected operational levels (200 ppm or less). This type of aging can be used independently, or combined with temperature cycling for aging tests. The history of the resonator frequencies during aging tests can be used for determining the utility of "pre-aging" to improve long-term stability. For example, if the resonator frequency shifts early in the aging test, but remains stable thereafter, then the strain and thermal cycling can be used as part of the fabrication process to attain the required stability.

The use of a single layer in fabrication of the resonator structure is not a fundamental limitation of the approach. The intent is to begin the investigation with the simplest approach. If single-layer resonators do improve stability characteristics, then one should consider multilayer structures as well. They offer more degrees of freedom in optimization of the design. There are other possible benefits that could accrue from using stiffening and loading layers in combinations that improve resonator Q-factor, as well. The approaches for using these other degrees of freedom will depend on the results from the single-layer designs.

2.5 Experimental Results

To measure the effects of passivation layers (thin films) on SAW resonators, a semiautomatic data acquisition system was used in conjunction with a Perkin-Elmer sputtering system. Conventional planar sputtering was used with the cryogenically pumped vacuum chamber. Depending on the material being

sputtered, either pure argon, nitrogen, or an argon/oxygen gas mixture was used, nominally at a pressure of 10 millitorr.

SAW resonators were fabricated at nominally 400 MHz (8.128 micron wavelength) and their electrical characteristics monitored via an HP 8505 network analyzer (phase locked to a frequency synthesizer). The data acquisition was automated with an HP 9825 calculator which analyzed the measured scattering parameters and calculated resonator series resonant frequency, equivalent resistance, and resonator Q. These were plotted versus time (derived from a system clock) as the deposition was taking place.

During sputtering of the passivation films temperature in the resonator fixture was measured and is shown in Fig. 15. The maximum temperature reached was a function of sputtering power, time, gas pressure, and target type. In all runs made the maximum temperature was never allowed to exceed 180°C.

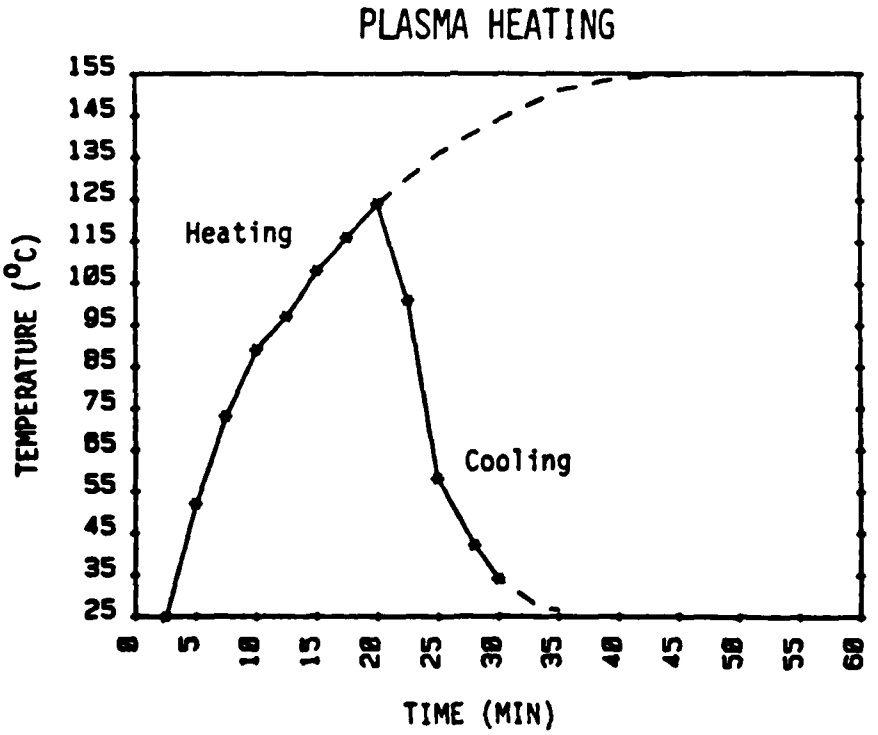

Fig. 15 Plasma temperature as a function of time in sealed SAW resonator during rf sputtering.

The SAW resonators were fabricated on rotated Y-cut quartz and had a parabolic temperature characteristic with a turning point at 75°C and a coefficient of 3.18×10^{-2} ppm/C^2. The effect of temperature was measured using resonators hermetically sealed in TO-5 enclosures. Shown in Fig. 16 is a plot of a typical resonator frequency, resistance and Q vs time during a sputtering run of SiO_x over a period of time equal to 30 min. After 20 min the sputtering was stopped and the system vented so as to return to room temperature. In general the effect of temperature was increased resistance, reduced Q and reduced frequency. These effects were reversible as shown.

Thin film passivation effects had been studied for a number of different materials. Results of interest were presented in previous reports. Among the different passivation materials Y_2O_3 and AlN were found to be the best passivation films. Effects of these films in resonator characteristics during the deposition are shown in Figs. 17 and 18. In both cases the sputtering rate was such that a film thickness of approximately 1000Å was achieved at the end of the deposition cycle.

A shown in each figure, the run was initiated at room temperature and atmospheric pressure. Pump-down to the vacuum required for sputtering resulted in drop in resistance and an increase in Q. This was to be expected since air loading results in lower Q. Sputtering was initiated approximately 15 min after pump-down and in all cases a rapid drop in Q and increase in resistance was observed due to heating effects discussed above. This was then followed by the loading effect of the film itself. After a period of time (equivalent to a 1000Å deposition), the sputtering unit was turned off and the system was vented to rapidly cool to room temperature.

The effect of film quality was clearly evident by the resonator resistance and Q. To date the best passivation film was found to be Y_2O_3. As shown in Fig. 17 the dispersion was large and linear, and the small increase in resistance and Q degradation were mostly due to temperature. This film appeared to be an excellent passivation material for SAW devices. AlN film indicates high resistive losses but has several interest points: 1) film has higher acoustic velocity therefore it has a positive temperature slope, 2) the film is also piezoelectric and in some cases this property can be used to an advantage.

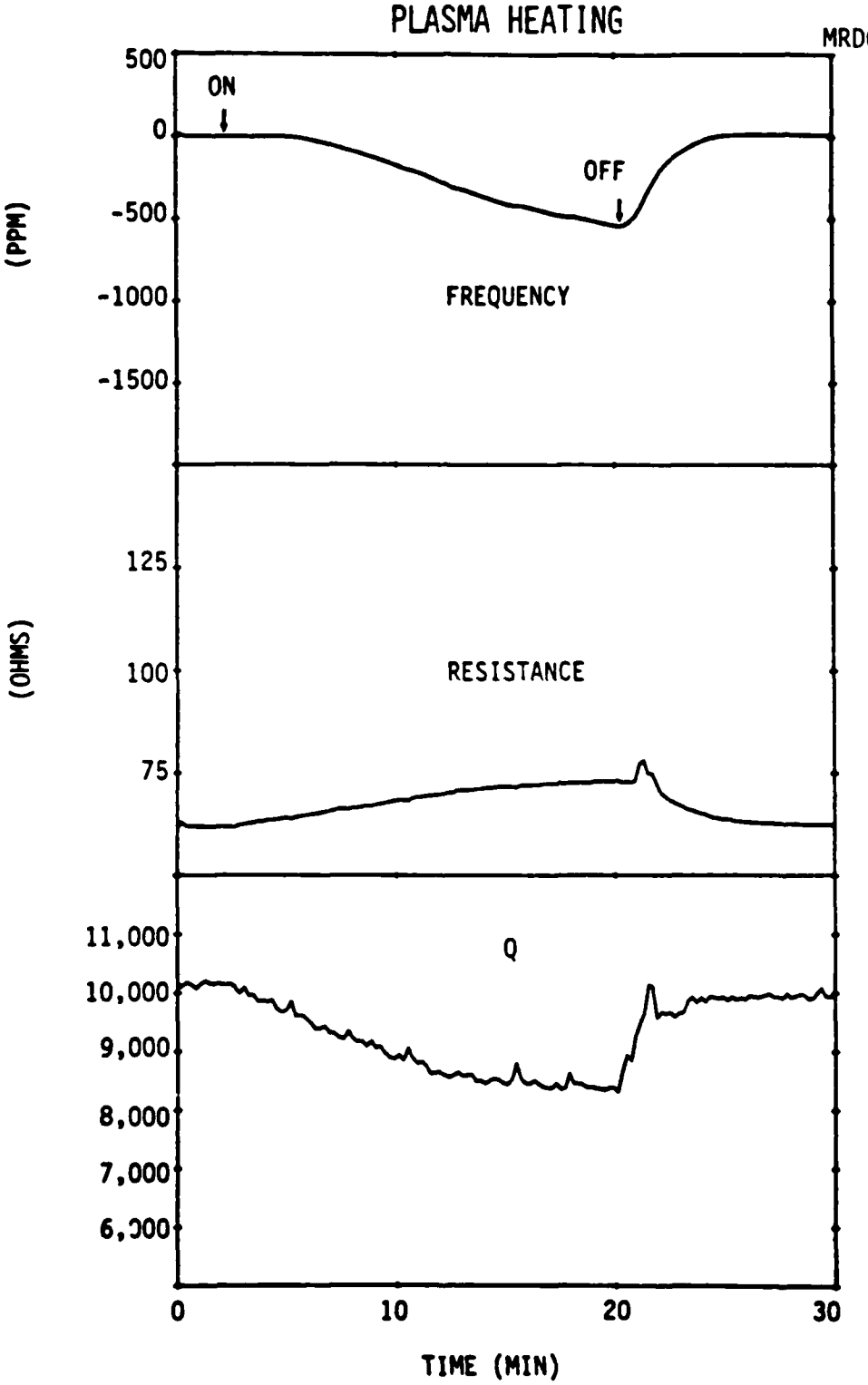

Fig. 16 Resonant frequency, resistance and Q vs time for hermetically sealed SAW resonator in RF plasma.

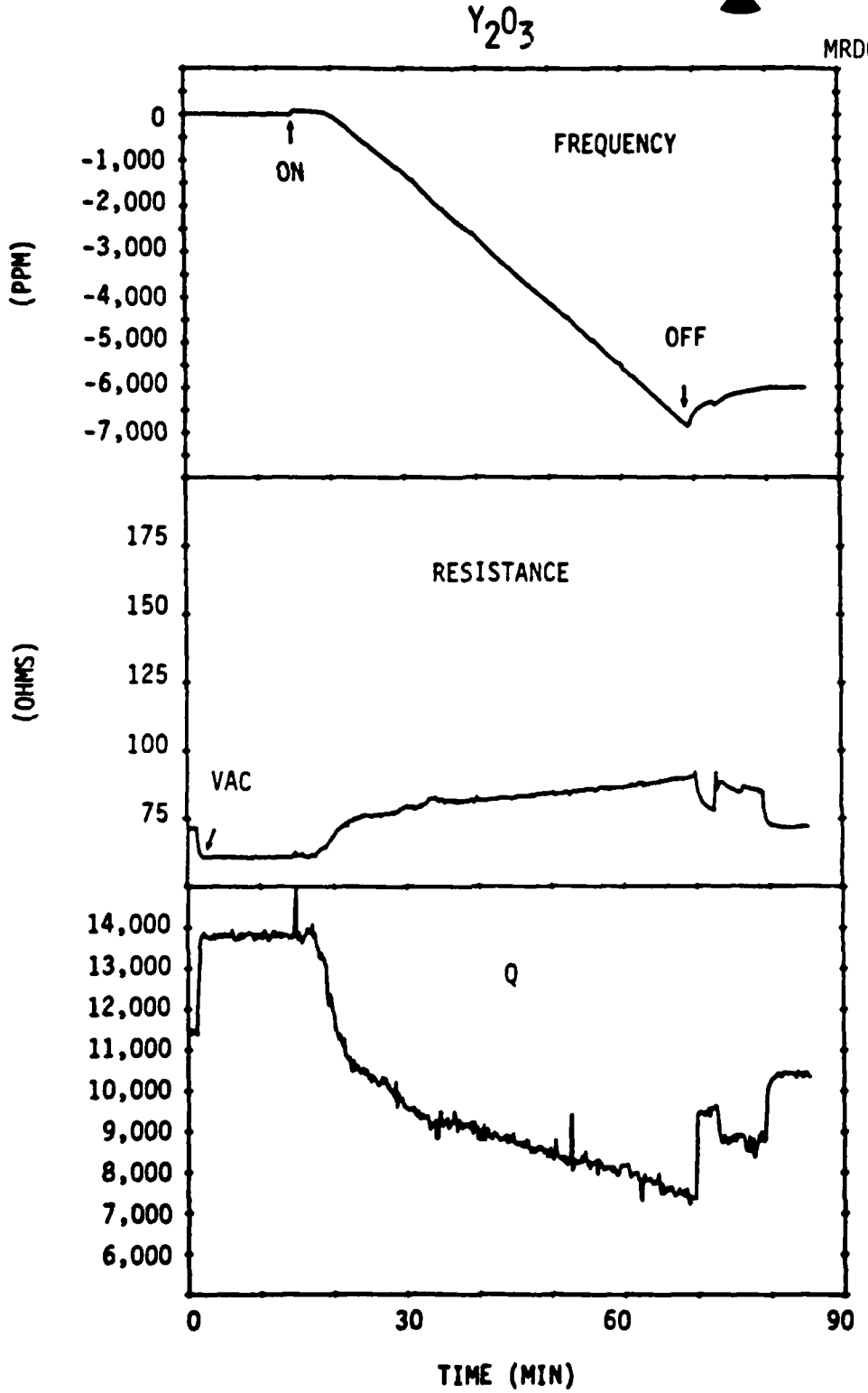

Fig. 17 Characteristics of SAW resonator during passivation of Y_2O_3 film.

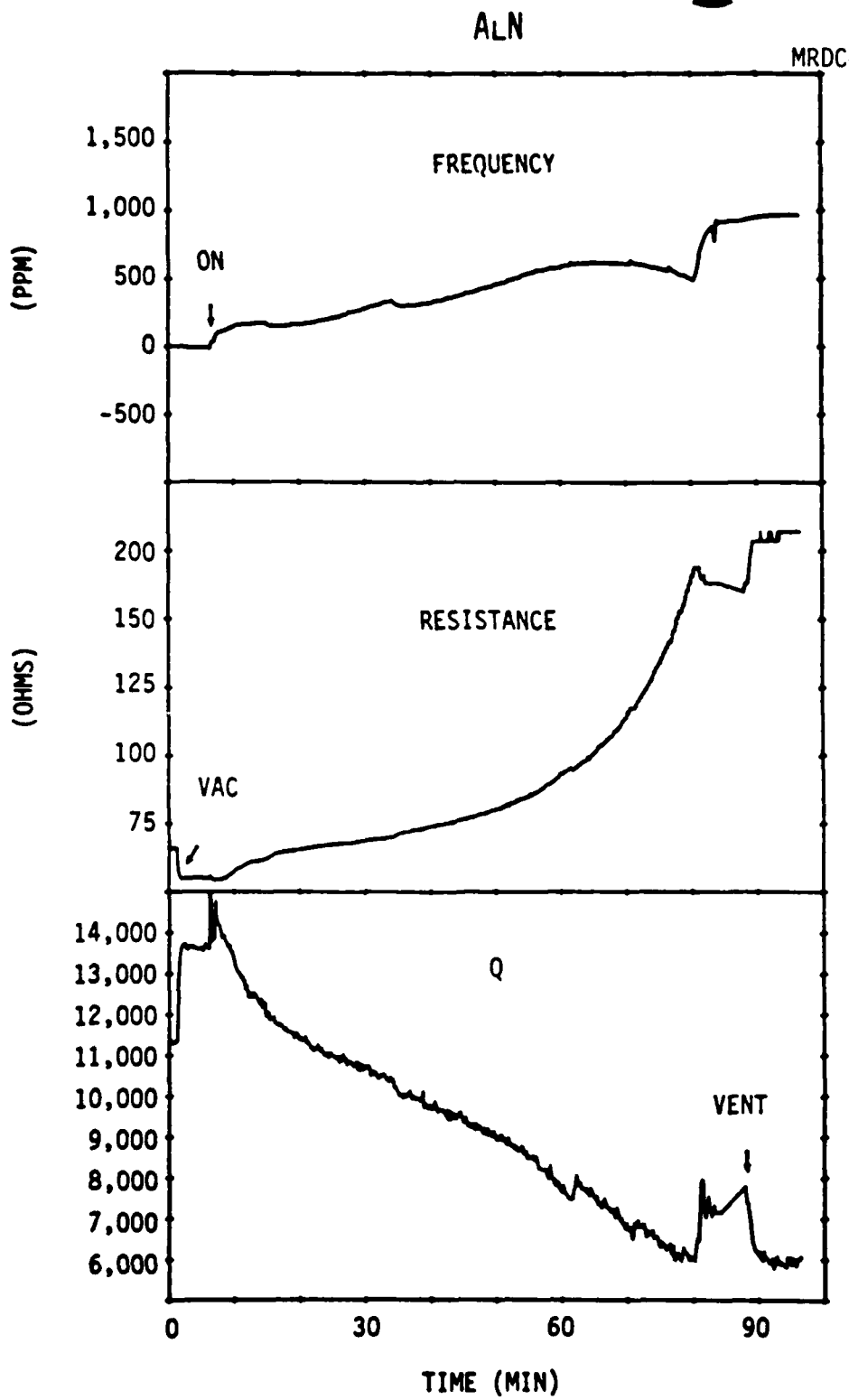

Fig. 18 Characteristics of SAW resonator during passivation of AlN film.

3.0 CONCLUSION

Methods of fabricating interface-wave single layered SAW resonator with low absolute and differential aging characteristics have been developed. Also, hybrid oscillator circuitry has been studied for the purpose of demonstrating acceleration sensing using interface-wave SAW resonator as a sensing element. To provide the desired accuracy, a quartz beam is designed with the required sensitivity and a size adequate for the resonator structure. A theory of the interface waves is developed for the purpose of material and thickness selection of passivation layers. Preliminary results indicated that Y_2O_3 (yttrium oxide) and AlN (aluminum nitride) were the best materials for passivation of the SAW resonators. A computer aided and completely automated system was developed for SAW sensor characteristics and aging data. An RF package with 50-ohm transmission lines was designed and fabricated to vacuum seal the entire oscillator and accelerometer hybrid circuitry.

4.0 FUTURE PLANS

The future plan is proposed to fabricate dual-resonator crystals with low absolute and differential aging with high stability less than 1×10^{-10} for a second averaging time. Twin oscillators will be fabricated to track in temperature to achieve bias stability and temperature insensitivity. Both Y_2O_3 and AlN will be used for passivation layers. A fabrication technique will be developed for two-sided alignment of interface-wave accelerometers at two-layered surface on quartz substrates. These accelerometers, fabricated by this technique, show high sensitivity and a better control in aging characteristics. To increase the sensitivity to a range of submicro-G, a one-dimensional proof mass will be designed during a beam shaping process prior to process of the SAW resonator structure.

5.0 REFERENCES

1. A.P. Andrews and M.E. Motamedi, "Monolithic Accelerometer," final report, Contract No. DASG60-79-C-0021, September 1983.

2. R.H. Parvin, Inertial Navigation, D. Van Nostrand, Princeton, NJ, 1962, p. 5.

3. J.M. Slater, "Which Accelerometers for Space Guidance?," Space/Aeronautics, October, 1960, pp. 227-240.

4. G.M. Siouris, "Survey of New Inertial Sensor Technology," Flugwiss Weltraumforsch, Vol. 1, No. 5, September-October, 1977, pp. 346-353.

5. W.C. Rosvold and M.L. Stephens, "Cantilever Accelerometer," AFAL-TR-77-152, WPAFB, OH, 1977.

6. P. Chen, R.S. Muller, T. Shiosaki and R.M. White, "Silicon Cantilver Beam Accelerometer Utilizing a PI-FET Capacitive Transducer," presented at Device Research Conference, Boulder, CO, 1979.

7. J.F. Dias, H.E. Karrer, "Stress Effects on Acoustic Surface-Wave Circuits and Applications to Pressure and Force Transducers," presented at 1975 IEEE International Solid-State Circuits Conference.

8. J.F. Dias and H.E. Karrer, "Stress Effects on Acoustic Surface-Wave Circuits and Applications to Pressure and Force Transducers," presented at 1975 IEEE International Solid-State Circuits Conference.

9. Lord Rayleigh, London Mathematic Society Proceedings, 17, 4 (1887).

10. W.M. Ewing, W.S. Jardetzky and F. Press, "Elastic Waves in Layered Media, " McGraw-Hill, 1957.

11. T.C. Lim and M.P. Musgrave, "Stoneley Waves in Anisotropic Media," Nature, Vol. 225, 1970, p. 372.

12. R. Stoneley, "Elastic Waves at the Surface of Separation of Two Solids," Proc. Royal Soc. (London), Vol. A245, 1924, p. 213.

13. G.W. Farnell and E.L. Adler, "Elastic Wave Propagation in Thin Layers," in Physical Acoustics, Vol. IX, edited by W.P. Mason and R.N. Thurston, Academic Press, 1972.

END

FILMED

6-85

DTIC